Demonstration of a 10-Hz Femtosecond-Pulse-Driven XUV Laser at 41.8 nm in Xe IX

B. E. Lemoff, G. Y. Yin, C. L. Gordon III, C. P. J. Barty, and S. E. Harris
Edward L. Ginzton Laboratory, Stanford University, Stanford, California 94305
(Received 1 July 1994)

We report the observation of a gain of approximately exp(11) at 41.8 nm in 8-times-ionized xenon. This extreme ultraviolet (XUV) laser is driven by a 10-Hz, 70-mJ circularly polarized femtosecond laser pulse. The laser is focused into Xe at pressures ranging from 5 to 12 torr. The laser is collisionally excited, with both the ions and electrons produced by field induced tunneling.

PACS numbers: 42.55.Vc, 32.30.Rj, 42.60.By, 52.50.Jm

Almost ten years ago, Matthews *et al.* [1], working at the Lawrence Livermore National Laboratory, reported laser amplification at wavelengths of 20.6 and 21.0 nm in Se XXV. The Se laser, and others like it [2], operate by sequential ionization of the target species until a closed shell is reached, followed by electron collisional excitation from the ionic ground state to the upper laser level. At the same time, Suckewer *et al.* [3], working at Princeton University, reported laser amplification at 18.2 nm in C VI. The carbon laser operates by fully ionizing the target species by sequential ionization, followed by recombination into the upper laser level. Both schemes required solid-density targets and pump laser pulse energies of several hundred joules. There has since been substantial effort and progress in reducing the necessary pump energy [4–6]. In related work, Rocca *et al.* [7], using a capillary discharge, have demonstrated lasing at 46.9 nm in Ar IX.

In this Letter we report the demonstration of a new class of extreme ultraviolet (XUV) lasers in which an intense circularly polarized femtosecond laser pulse is used to tunnel ionize a gaseous target species while simultaneously producing the hot electrons necessary to collisionally excite the species. Corkum and Burnett first suggested pumping a collisionally excited laser in this way [8], while the first specific systems were proposed by Lemoff, Barty, and Harris [9], who gave calculations for lasing in Ar IX (Ne-like), Kr IX (Ni-like), and Xe IX (Pd-like). We have observed lasing at 41.8 nm on the $4d^95d\,^1S_0$-$4d^95p\,^1P_1$ transition in Xe IX. A 10-Hz, 800-nm laser pulse with an energy of ~70 mJ and time duration of ~40 fs is longitudinally focused in a differentially pumped cell containing 5 to 12 torr of Xe gas. Laser amplification was observed with an estimated gain coefficient of 13 cm^{-1} and a total gain of exp(11). To our knowledge, this is the highest gain ever observed in a tabletop laser system operating below 90 nm. This is also the first XUV laser to operate at a 10-Hz repetition rate and the first that does not require a solid target.

A partial energy level diagram of Xe IX is shown in Fig. 1. The energies of the $4d^95p\,^1P_1$ and $4d^94f\,^1P_1$ levels are obtained from published data [10]. The designation and energies of the remaining levels were obtained from our own spectroscopic studies in conjunction with the RCN/RCG atomic physics code [11]. The ions are created by the optical pulse through tunneling ionization, where ionization rates vary exponentially with laser intensity. Using tunneling ionization formulas [12] and an estimated focal intensity of 3×10^{16} W/cm^2, the tunneling rate from neutral Xe to Xe IX is 1.5×10^{17} s^{-1}. The ionization rate from Xe IX to Xe X is 5×10^5 s^{-1}, and is thus inconsequential. We thus expect a 40-fs pulse to produce, over some volume, a nearly uniform plasma of Xe IX. Following the ideas of Corkum and co-workers [8,13], we expect that as the circularly polarized laser pulse ends, the electrons will retain a kinetic energy which is equal to the quiver energy $\varepsilon = e^2E^2/4m\omega^2$ at the time of ionization. This is necessary to satisfy conservation of angular momentum or, equivalently, zero velocity at the instant of ionization. This energy varies from ~9 for the first electron ionized to ~550 eV for the eighth electron ionized [9]. The last four electrons ionized are expected to have energies greater than 104 eV, thus contributing to collisional excitation of the upper laser level. Because no collisions occur during the short optical pulse,

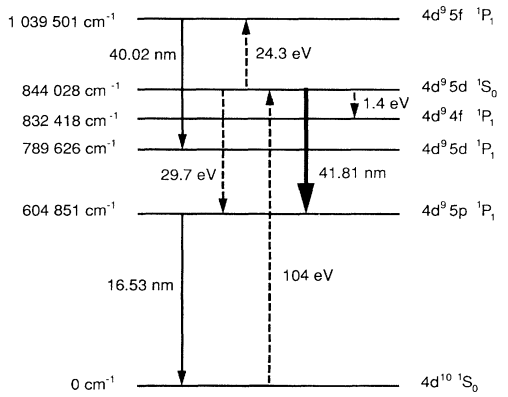

FIG. 1. Partial energy level diagram of Xe IX, showing observed lines at 16.53 nm, 40.02 nm, and the laser line at 41.81 nm. The dashed lines indicate the dominant collisional excitation and deexcitation channels of the upper laser level.

 0031-9007/95/74(9)/1574(4)$06.00

the ions remain very near to room temperature. The laser line is therefore believed to be predominantly Stark broadened. At 12 torr, we estimate the laser transition to have a linewidth of ~0.001 nm [14]. The plasma is calculated to be optically thick at 16.53 nm, with an absorption length at 12 torr of 0.06 μm. Thus the lower laser level will be trapped, forcing stimulated emission to self-terminate after one upper-state lifetime (~30 ps for pressures <1 torr, ~3.4 ps at 12 torr).

The femtosecond laser system used in this experiment is the Ti:sapphire chirped pulse amplification system described in Ref. [15]. The 40-fs, 800-nm pulse is passed through a 1.6-in.-diameter, 5-mm-thick MgF_2 window into an evacuated chamber where a 2-in.-diamter, 41-μm-thick mica quarter waveplate produces a circularly polarized beam, which is focused by a 50-cm focal length mirror into a differently pumped Xe cell. The pulse energy reaching the Xe is ~70 mJ. It was not possible to directly measure the focused spot size under the conditions of the experiment, in which the plasma is likely to affect beam propagation [9]; however, from the observed ion stages we can deduce that the peak intensity was higher than 3×10^{16} W/cm^2 over a length of at least 7.4 mm. With a highly attenuated beam propagating in air, we measured an astigmatic focus with area less than 5×10^{-5} cm^2 over a distance of ~1 cm. We thus estimate that the gain region is between 50 and 100 μm in diameter over most of its length.

A diagram of the target cell is shown in Fig. 2. This cell, together with the gas supply line, has a volume of approximately 7 liters, and is held at a constant, uniform pressure. Two replaceable pinholes of diameter <500 μm, whose separation can be varied by means of translation stages, provide the entrance orifice for the pump laser and the exit orifice for both the pump and XUV lasers. These pinholes are drilled *in situ* in 0.004-in.-thick brass stock by the femtosecond laser pulse. At a cell pressure of 12 torr of Xe, the background pressure in the continuously pumped vacuum chamber is less than 2 mtorr. The femtosecond laser pulse thus propagates in a nearly gas-free region until it reaches the region immediately outside of the entrance pinhole.

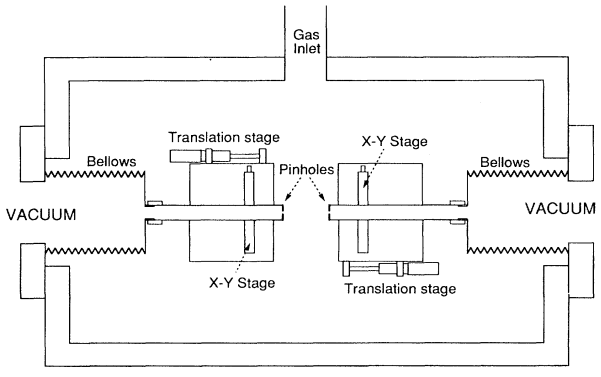

FIG. 2. Schematic diagram of differentially pumped target cell. The cell sits inside of a larger vacuum chamber.

Although the pinhole translation stages allow accurate measurement of changes in pinhole separation, the determination of the effective lasing length is more complicated and depends on the pressure distribution outside of the pinholes, as well as the focusing properties of the pump laser. To estimate the absolute length, we measure the 41.8-nm signal versus pinhole separation with the pressure below 3 torr, where the signal varies linearly with length, and extrapolate to zero signal. Throughout this Letter, we assume that the effective length is independent of pressure; however, because of beam propagation effects, this may not be a valid assumption at higher pressure.

The XUV radiation escaping from the target cell enters a 1.5-m grazing incidence monochromator (Acton Research Corp. model GIMS-551.5-M) whose entrance slit is located ~62 cm from the center of the target cell. Entrance and exit slits are 20 μm wide and 1 cm high, and the grating has a groove density of 1200 lines/mm. The spectrometer was calibrated using the 25.632-nm line of He II [16] and 16.533-nm line of Xe IX [10] and has an accuracy of 0.01 nm and a resolution of ~0.035 nm in the vicinity of 40 nm. The signal is detected by a dc-biased, double microchannel plate located behind the exit slits, followed by an rf preamplifier (Phillips Scientific model 6954B-100) and a boxcar integrator (Stanford Research Systems model 250) with a 5-ns time gate. Because the dynamic range of our measurements exceeds that of the detector at a fixed bias voltage, several voltages were used. All voltage data have been normalized to be directly compared to a signal corresponding to a microchannel plate bias of 2000 V.

Lasing at 41.81 nm is evident in the dependence of the signal on both pressure and length. The most convenient parameter to adjust is pressure. Figures 3(a) and 3(b) show spectral scans in the vicinity of 41.8 nm and a length of 8.4 mm at Xe pressures of 3 and 12 torr, respectively. The 3-torr scan shows three prominent lines: The 40.02-nm line corresponds to the Xe IX $4d^9 5f\,{}^1P_1$-$4d^9 5d\,{}^1P_1$ transition (see Fig. 1), the 41.45-nm line may be the $5s5p\,{}^3P_2$-$5s6s\,{}^3S_1$ line of Xe VII [17], and the 41.81-nm line corresponds to the laser transition. The 12-torr spectrum has a dynamic range of 40. No lines other than 41.81 nm are visible.

Figure 4 shows the 41.81-nm signal at a length of 8.4 mm as the pressure is continuously varied from 0 to 10 torr. Doubling the pressure from 4 to 8 torr increases the signal by a factor of 80. For comparison, Fig. 5 shows the (nearly linear) dependence of the emission at 40.02 and 16.53 nm. The extent of the dependence on pressure is somewhat obscured by the 5-ns time gate. At 1 torr, stimulated emission is expected to terminate 30 ps following ionization, while spontaneous emission

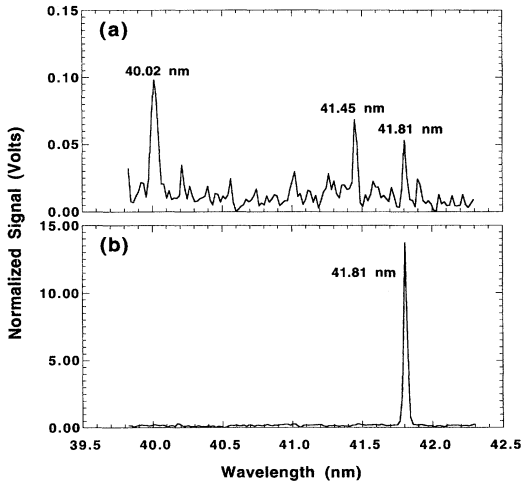

FIG. 3. Observed emission spectrum at an estimated length of 8.4 mm and a pressure of (a) 3 torr and (b) 12 torr. Note the factor of 100 scale change between the two plots.

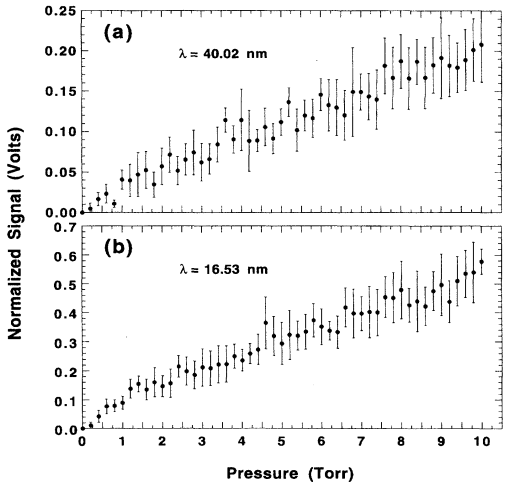

FIG. 5. Pressure dependence at an estimated length of 8.4 mm of the observed line emission at (a) 40.02 nm and (b) 16.53 nm.

is observed to continue for longer than the 5-ns gate width. The observed ratio of the 41.81-nm signal at 10 torr to that at 1 torr is ~700. If the 1-torr signal is primarily spontaneous emission, a 30-ps time-gated measurement would reveal a ratio of greater than 10^5, which is consistent with a gain greater than exp(10). Note that we have not measured the XUV laser pulse duration.

Varying length provides a more direct measure of stimulated gain. To vary the length, the vacuum chamber must be vented and opened and the pinhole separation changed. Figure 6 shows the 41.81-nm signal at a pressure of 12 torr and several lengths ranging from 3.9 to 8.4 mm. For this set of data, only the exit pinhole position was changed. Each data point represents an average of over ~3000 shots. Also shown (solid line) is the best fit by the Linford expression [18]

$$I \sim [\exp(gL) - 1]^{3/2}/[gL\exp(gL)]^{1/2}.$$

From this fit, the differential gain is estimated to be $13.3 \pm 0.9\ \mathrm{cm}^{-1}$. At an effective length of 8.4 mm, our best estimate of the total gain is exp(11.2). When a Linford curve is fit only to the data from 3.9 to 7.4 mm (dashed line), a better fit is obtained with $g = 16.8 \pm 0.5\ \mathrm{cm}^{-1}$. Assuming a length of 7.4 mm, we obtain a gain of exp(12.4).

Using the model of Ref. [9], the predicted differential gain is $163\ \mathrm{cm}^{-1}$, approximately 1 order of magnitude

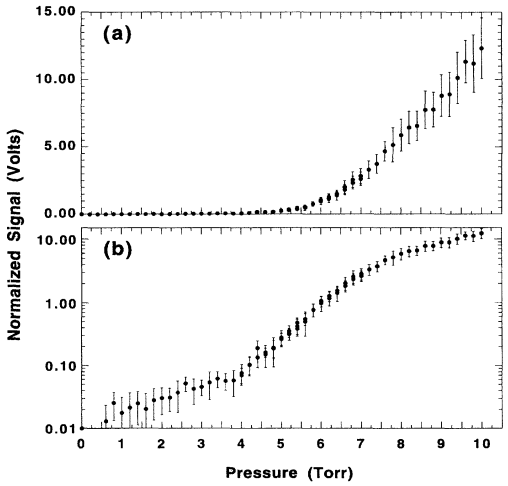

FIG. 4. Pressure dependence at an estimated length of 8.4 mm of the observed 41.81-nm line emission: (a) linear scale, (b) logarithmic scale.

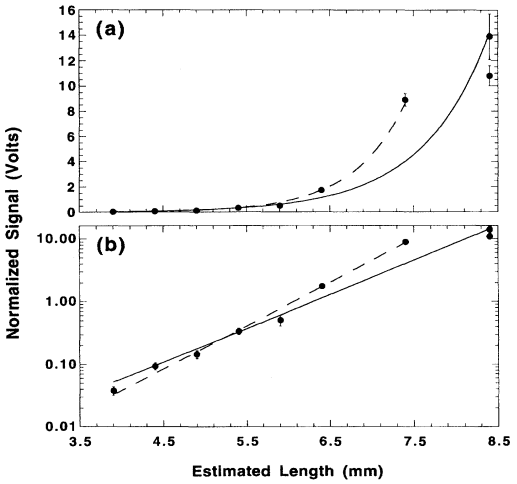

FIG. 6. Length dependence at a pressure of 12 torr of the observed 41.81-nm line emission. Linford curves are shown to fit to all the data (solid line) and 3.9 through 7.4 mm only (dashed line): (a) linear scale, (b) logarithmic scale.

higher than that observed. One possible reason for the discrepancy is that the model did not take into account the fact that many of the high energy electrons may leave the gain region in a time shorter than the upper state lifetime, thus reducing the number of electrons available to pump the laser. Further experimental study will be necessary before this question can be resolved. It should be noted that because of the low gas density, pump beam dispersion and depletion over the gain length are negligible.

This work has demonstrated a new approach to short wavelength lasers. The essence of this approach is the use of very intense, circularly polarized pumping radiation to simultaneously produce a cold, highly ionized target species and a very hot electron distribution. Scaling to shorter wavelengths will require higher laser intensities, and thus either higher pulse energies or a method of channeling a tightly focused pumping laser beam over a distance longer than its confocal parameter (perhaps using a hollow waveguide). As an example, a laser intensity of 5×10^{18} W/cm^2 should produce Xe XXVII (Ni-like), which would have a lasing wavelength of $\sim$10 nm.

The authors gratefully acknowledge the assistance of P. T. Epp and J. J. Macklin. This work was supported by the Air Force Office of Scientific Research, the Army Research Office, and the Ballistic Missile Command.

[1] D. L. Matthews, P. L. Hagelstein, M. D. Rosen, M. J. Eckart, N. M. Ceglio, A. U. Hazi, B. J. MacGowan, J. E. Trebes, B. L. Whitten, E. M. Campbell, C. W. Hatcher, A. M. Hawryluk, R. L. Kauffman, L. D. Pleasance, G. Rambach, J. H. Scofield, G. Stone, and T. A. Weaver, Phys. Rev. Lett. **54**, 110 (1985).

[2] B. J. MacGowan, S. Maxon, C. J. Keane, R. A. London, D. L. Matthews, and D. A. Whelan, J. Opt. Soc. Am. B **5**, 1858 (1988).

[3] S. Suckewer, C. H. Skinner, H. Milchberg, C. Keane, and D. Voorhees, Phys. Rev. Lett. **55**, 1753 (1985).

[4] C. H. Skinner, D. Kim, D. Voorhees, and S. Suckewer, J. Opt. Soc. Am. B **7**, 2042 (1990).

[5] S. Basu, P. L. Hagelstein, J. G. Goodberlet, M. H. Muendel, and S. Kaushik, App. Phys. B **57**, 303 (1993).

[6] Y. Nagata, K. Midorikawa, S. Kubodera, M. Obara, H. Tashiro, and K. Toyoda, Phys. Rev. Lett. **71**, 3774 (1993).

[7] J. G. Rocca, V. Shlyaptsev, F. Tomesel, and O. Cortzar (to be published).

[8] P. B. Corkum and N. H. Burnett, in *OSA Proceedings on Short Wavelength Coherent Radiation: Generation and Applications,* edited by R. W. Falcone and J Kirz (Optical Society of America, Washington, DC, 1988), Vol. 2, p. 225.

[9] B. E. Lemoff, C. P. J. Barty, and S. E. Harris, Opt. Lett. **19**, 569 (1994).

[10] J. Sugar and V. Kaufman, Phys. Scr. **26**, 419 (1982).

[11] R. D. Cowan, *The Theory of Atomic Structure and Spectra* (University of California, Berkeley, 1981), Secs. 8-1, 16-1, and 18-13.

[12] N. H. Burnett and P. B. Corkum, J. Opt. Soc. Am. B **6**, 1195 (1989).

[13] P. B. Corkum, N. H. Burnett, and F. Brunel, Phys. Rev. Lett. **62**, 1259 (1989).

[14] M. S. Dimitrijevic and N. Konjevic, in *Spectral Line Shapes,* edited by B. Wende (W. de Gruyter, Berlin, 1981), p. 211.

[15] C. P. J. Barty, C. L. Gordon III, and B. E. Lemoff, Opt. Lett. **19**, 1442 (1994).

[16] R. L. Kelly, J. Phys. Chem. Ref. Data **16**, Suppl. 1, 21 (1987).

[17] V. Kaufman and J. Sugar, J. Opt. Soc. Am. B **4**, 1919 (1987).

[18] G. J. Linford, E. R. Peressini, W. R. Sooy, and M. L. Spaeth, Appl. Opt. **13**, 379 (1974).